

## Accepted Manuscript

Interfacial Microstructure and Shear Strength of Ti-6Al-4V/TiAl Laminate Composite Sheet Fabricated by Hot Packed Rolling

Fantao Kong, Yuyong Chen, Deliang Zhang

PII: S0261-3069(11)00143-9  
DOI: [10.1016/j.matdes.2011.02.052](https://doi.org/10.1016/j.matdes.2011.02.052)  
Reference: JMAD 3621

To appear in: *Materials and Design*

Received Date: 4 November 2010  
Accepted Date: 22 February 2011

Please cite this article as: Kong, F., Chen, Y., Zhang, D., Interfacial Microstructure and Shear Strength of Ti-6Al-4V/TiAl Laminate Composite Sheet Fabricated by Hot Packed Rolling, *Materials and Design* (2011), doi: [10.1016/j.matdes.2011.02.052](https://doi.org/10.1016/j.matdes.2011.02.052)

This is a PDF file of an unedited manuscript that has been accepted for publication. As a service to our customers we are providing this early version of the manuscript. The manuscript will undergo copyediting, typesetting, and review of the resulting proof before it is published in its final form. Please note that during the production process errors may be discovered which could affect the content, and all legal disclaimers that apply to the journal pertain.



**Interfacial Microstructure and Shear Strength of  
Ti-6Al-4V/TiAl Laminate Composite Sheet Fabricated  
by Hot Packed Rolling**

Fantao Kong<sup>a,c,\*</sup>, Yuyong Chen<sup>a</sup>, Deliang Zhang<sup>b</sup>

*<sup>a</sup>School of Materials Science and Engineering, Harbin Institute of Technology, Harbin  
150001, R.P.China*

*<sup>b</sup>Waikato Centre for Advanced Materials (WaiCAM), School of Engineering, The  
University of Waikato, Private Bag 3105, Hamilton, New Zealand*

*<sup>c</sup>State Key Laboratory of Advanced Welding Production Technology, Harbin Institute of  
Technology, Harbin 150001, R.P.China*

\* Corresponding author, Email: kft@hit.edu.cn (Fantao Kong)

Tel: +86 451 86418802, Fax: +86 451 86418802

# Interfacial Microstructure and Shear Strength of Ti-6Al-4V/TiAl Laminate Composite Sheet Fabricated by Hot Packed Rolling

Fantao Kong<sup>a,c,\*</sup>, Yuyong Chen<sup>a</sup>, Deliang Zhang<sup>b</sup>

<sup>a</sup>*School of Materials Science and Engineering, Harbin Institute of Technology, Harbin  
150001, R.P.China*

<sup>b</sup>*Waikato Centre for Advanced Materials (WaiCAM), School of Engineering, The  
University of Waikato, Private Bag 3105, Hamilton, New Zealand*

<sup>c</sup>*State Key Laboratory of Advanced Welding Production Technology, Harbin Institute of  
Technology, Harbin 150001, R.P.China*

**Abstract:** A two layer Ti-6Al-4V(wt%)/Ti-43Al-9V-Y(at%) laminate composite sheet with a uniform interfacial microstructure and no discernible defects at the interfaces has been prepared by hot-pack rolling, and its interfacial microstructure and shear strength were characterized. Characterization of the interfacial microstructure shows that there was an interfacial region of uniform thickness of about 250  $\mu\text{m}$  which consisted of two layers: Layer I on the TiAl side which was 80  $\mu\text{m}$  thick and Layer II on the Ti-6Al-4V side which was 170  $\mu\text{m}$  thick. The microstructure of Layer I consisted of massive  $\gamma$  phases, needlelike  $\gamma$  phases and B2 phase matrix, while the microstructure of Layer II consisted of  $\alpha_2$  phase. The microstructure of the interfacial region is the result of the interdiffusion of Ti element from Ti-6Al-4V alloy layer into the TiAl alloy layer and Al element from the TiAl alloy layer into the Ti-6Al-4V alloy layer. The shear strength

measurement demonstrated that the bonding strength between the TiAl alloy and Ti-6Al-4V alloy layers in the laminate composite sheet was very high. This means that the quality of the interfacial bonding between the two layers achieved by the multi-path rolling is high, and the interface between the layers is very effective in transferring loading, causing significantly improved toughness and plasticity of the TiAl/Ti-6Al-4V laminate composite sheet.

**Keywords:** A. Intermetallics; B. Laminates; F. Microstructure

## 1. Introduction

Recently, laminate composites (LMCs), consisting of alternating laminates of different constitutive materials such as ceramic-ceramic [1], metal-ceramic [2], metal-metal [3], metal-ceramic-intermetallic [4] and metal-intermetallic [5] have been widely researched and applied. With optimum materials combinations and layer thickness designs, LMCs can possess various advantages such as low density, high corrosion resistivity, high strength, and high fracture toughness [6-9]. LMCs consisting of ductile metal and brittle intermetallic laminates have become increasingly attractive in recent years because of their low density, high stiffness, high strength and much improved ductility and toughness compared with the intermetallic material [10,11]. In metal-intermetallic based LMCs, the interface quality and bonding strength play a critically important role in controlling their mechanical properties. Weak interfacial

bonding can result in preferential crack initiation at interfaces and, hence, reduce the strength, toughness and ductility of the composite. It has been suggested that strong interfaces in LMCs are characterised by ductile interfacial reaction layers with a suitable thickness [12-15].

Intermetallic alloys based on Ti-Al system have potential as high temperature materials for the application of aerospace and automobile engine [16-18]. Metal-intermetallic based LMCs with Ti-Al based intermetallics, such as the Ti-Al<sub>3</sub>Ti system with alternate layers of Al<sub>3</sub>Ti and residual Ti prepared by diffusion bonding of Ti and Al metal foils, being the reinforcing phase has also been investigated with promising results [19-21]. However, this processing method may cause small voids at the region near the interface or in the intermetallic layer because of metal shrinkage during interdiffusion or reaction between Ti and Al metal foils, which results in the decreasing of mechanical properties.

For manufacturing LMCs, rolling process is the most efficient and economical technique [10,15,22]. Hot roll bonding is a solid-state welding process in which double or multiple layers of metal and/or alloys are stacked together and rolled to cause enough deformation to produce solid-state welds. Hot roll bonding can also improve strengths of the individual constituent materials by refining their microstructures, leading to a much enhanced overall strength of the laminated composite compared with individual materials. Our previous research has shown that a LMC consisting of TiAl alloy and Ti-6Al-4V (wt%) (Ti64) laminates can be fabricated by hot roll bonding and has

excellent mechanical properties [23]. It is expected that the bonding state at interfaces between the Ti64-TiAl laminates plays a critical role in determining the mechanical behavior of composite laminates. However, no experimental and theoretical studies of interfacial structures and mechanical properties in Ti alloy-TiAl based LMCs have been reported. There is a compelling need to understand the interfacial microstructure and bonding strength of Ti alloy-TiAl LMCs which are critical in developing high-performance Ti alloy-TiAl LMCs. In this study, we investigated the interfacial microstructure and shear strength of a Ti64-TiAl LMC consisting of two layers and prepared by hot roll bonding.

## 2. Experimental Procedure

To prepare the Ti64-TiAl LMC sheet, a 10 mm thick TiAl alloy plate was cut from a TiAl alloy pancake which had a composition of Ti-42.8Al-8.8V-0.21Y (at%) with the oxygen content being <500ppm and have been prepared by a combination of ingot casting, homogenization, hot isostatic pressing and hot forging [24]. The TiAl plate and a 3 mm thick sheet of Ti-6Al-4V (wt%) alloy were stacked together after their surfaces were ground and cleaned. The TiAl plate/Ti-6Al-4V sheet stack was placed in a stainless steel can which was then sealed. The canned sample was hot-rolled after it was heated to 1180°C and held at the temperature for 1 hour in a furnace. The canned sample was hot rolled through fifteen passes with the nominal thickness reduction per pass being approximately 10% and the nominal rolling speed being approximately

0.5m/s. Between consecutive passes, the canned sample was re-heated back to 1180°C and held at the temperature for 10-15 minutes. Following the last pass of rolling, the rolled sheet was furnace cooled and then decanned. The Ti64-TiAl LMC sheet did not show any cracks and had a thickness of 2.9mm which corresponded to a total thick reduction of about 78%. The thickness of TiAl alloy layer and Ti64 alloy layer was 2.3 and 0.6mm, respectively.

The microstructures of the LMC sheet produced by hot rolling were examined using X-ray diffractometry (XRD), scanning electron microscopy (SEM) in conjunction with energy dispersive X-ray spectrometry (EDS) and transmission electron microscopy (TEM). The XRD was carried out using Cu K $\alpha$  radiation ( $\lambda= 0.154157$  nm) and  $2\theta$  ranging from 20° to 100°. Specimens for TEM observation were prepared using a standard procedure and an electrolytic jet polisher with the electrolyte being a solution of 60% methanol, 35% n-butyl alcohol and 5% perchloric acid. The interfacial shear test samples, as schematically shown in Fig.1, were prepared by spark erosion parallel to the rolling direction. The samples were tested at a strain rate of  $5\times 10^{-3}\text{s}^{-1}$  at room temperature by using a tensile testing machine. The shear strength was calculated using the following equation.

$$\tau = \frac{F}{b \times w} \quad (1)$$

Where  $\tau$  is ultimate shear strength (MPa),  $F$  is maximum shear load (N), and  $b$  and  $w$  are sample length and width of the shear surface (mm), respectively.

### 3. Results and Discussion

#### 3.1 Microstructures

The microstructures of Ti-6Al-4V alloy and TiAl alloy layers of the composite sheet are shown in Fig.2. The TiAl alloy layer had an equiaxed near  $\gamma$  structure (NG) with the grain sizes in the range of 15-30  $\mu\text{m}$  (Fig. 2(a)). The microstructure of Ti-6Al-4V alloy layer consisted of  $\alpha/\beta$  lamellar colonies with sizes in the range of 50-150  $\mu\text{m}$  (Fig. 2(b)). XRD analysis of the TiAl layer showed that it composed of mainly  $\gamma$  and B2 phases and a small amount of  $\alpha_2$  phase. TEM examination of the specimens from the TiAl alloy layer showed that the dark equiaxed grains and plates shown in Fig. 2(a) were  $\gamma$  phase, and the grey blocks distributed along the boundaries between equiaxed grains were B2 phase. This indicates that complete recrystallization of the  $\gamma$  phase occurred during hot rolling, and led to formation of fine equiaxed  $\gamma$  grains. These results are similar to the previous results found in a study on hot rolling of the Ti-43Al-9V-Y alloy [24].

There was an interfacial region of uniform thickness of about 250  $\mu\text{m}$  between the TiAl layer and the Ti64 layer of the LMC sheet. SEM examination of this interfacial region (Fig. 3(a)) revealed no discernible defects such as cracks or voids at the interfaces. Based on the microstructure of the interfacial region, it contained two layers: Layer I which was 80  $\mu\text{m}$  thick and Layer II which was 170  $\mu\text{m}$  thick. Fig. 3(b) shows the distribution of the contents Ti, Al and V across the interfacial region, as determined using semi-quantitative EDS microanalysis technique. A continuous change in the



contents of Ti, Al and V along the line from A to B across the interfacial region as shown in Fig.3(a) was observed. This indicates that interdiffusion between the TiAl and Ti64 layers took place during hot rolling at 1180°C. The width of the interdiffusion zone is in good accordance with the thickness of the interfacial region determined based on the microstructural examination. XRD analysis of the cross-section of specimen (Fig. 4) showed that the LMC sheet was composed of  $\gamma$ ,  $\alpha_2$ , B2,  $\beta$  and  $\alpha$  phases. This reveals that no new phases formed at the interfaces during hot rolling.

Fig. 5 shows the SEM backscattered electron images of the microstructures of Layers I and II of the interfacial region between the TiAl and Ti64 layers. The SEM images of the microstructure of Layer I which was on the TiAl side showed four types of contrast: dark islands (A), dark grey blocks (B), dark needles (C) and grey matrix (D), as shown in Fig.5(a). EDS analysis results of these microstructural features are shown in Table 1. Based on the EDS analysis, it can be determined that the dark islands (A) and dark grey blocks (B) were  $\gamma$  phases with different V concentrations, the grey matrix (D) was B2 phase, and the dark needles (C) were also  $\gamma$  phase. Because V concentrations of the dark grey blocks is higher than that of the dark blocks and the dark needles, the color of position B is more light than that of the positions A and C in the SEM backscattering mode. The SEM images of the microstructure of Layer II which was on the Ti64 side showed only one kind of contrast, as shown in Fig.5(b). EDS data was collected from four points (as indicated by E, F, G, and H in Fig. 5(b)) along a horizontal line across Layer II, and are also shown in Table 1.

By comparing the EDS analysis results with the phase compositions ranges shown in the Ti-Al binary phase diagram [16, 18], the phases corresponding to the microstructural features in the interfacial region were identified, and also shown in Table 1. Fig. 6 shows representative TEM bright images of the microstructures of Layer I and Layer II of the interfacial region. As shown in Fig. 6(a), TEM examination of the interfacial region in conjunction with EDS analysis showed that Layer I was mainly composed of  $\gamma$  and B2 phases. In Layer I, the volume fraction of  $\gamma$  phases decreased and the volume fraction of B2 phases increased, both due to lowering of the Al content caused by the diffusion of Al atoms from the TiAl layer into the Ti64 layer. Due to the diffusion, the morphology of  $\gamma$  phase in Layer I also changed obviously from equiaxed shape into needle shape, and most of the needles grew towards the Ti64 layer. EDS analysis showed that the entire Layer II contained 20-31 at.% Al which falls into the composition range of the intermetallic compound  $DO_{19}$  type  $\alpha_2$ -Ti<sub>3</sub>Al according to the Ti-Al binary phase diagram [16,18]. This indicates that Ti<sub>3</sub>Al can be formed in this layer by a chemical reaction between titanium and aluminium. TEM observation of the interface microstructure of the interfacial region also confirmed that Ti<sub>3</sub>Al grains formed in layer II, as shown in Fig.6(b). Near the boundary Layer I and Layer II, B2 grains were also found (Fig. 6(b)). Thus, most of the prior phases in Layer II:  $\gamma$ ,  $\alpha$ ,  $\beta$  and B2 phases, were transformed into  $\alpha_2$ -Ti<sub>3</sub>Al during hot rolling. By combining the results of microstructural examination and compositional analysis, the structure of the interfacial region of the laminate composite sheet can be determined, as shown by the

schematic diagram in Fig. 7.

According to vertical sections of Ti–Al–V ternary system [25], during increasing temperature of the canned sample, phase transformations of Ti-43Al-9V-Y alloy took place along the pathway of  $\gamma+B2 \rightarrow \gamma+\beta \rightarrow \alpha+\gamma+\beta \rightarrow \alpha+\beta$ . The  $\beta$  phase became B2 by second order transition at about 1100 °C. Therefore, for Ti-43Al-9V-Y plate, the ordered B2,  $\gamma$  and  $\alpha_2$  phases present in the original plate changed into disordered  $\alpha$  and  $\beta$  phases at 1180°C before hot rolling. For Ti-6Al-4V alloy layer, the  $\alpha$  phase present in the original alloy was transformed into  $\beta$  phases before hot rolling [16]. During hot rolling at 1180°C, the interdiffusion between the TiAl layer (consisting of  $\alpha$  and  $\beta$  phases with high Al contents) and the Ti64 layer (consisting of only  $\beta$  phase with low Al content) took place due to the different of elemental contents. Compared with mobility of titanium, the mobility of aluminum is very high at elevated temperatures such as 1180°C [26], so the interfacial region growth presumably begins with the diffusion of aluminum atoms from the  $\alpha$  and  $\beta$  phases in the TiAl layer across the interface and into the  $\beta$  phases in the Ti64 layer, and then the diffusion of titanium atoms from the  $\beta$  phase in the Ti64 layer across the interface and into the  $\alpha$  and  $\beta$  phases in the TiAl layer. Therefore, the thickness of Layer II in the interfacial region is larger than that of Layer I. The region near the boundaries between Layer I and Layer II may be the original contact surface of the constituent materials. Due to the rapid diffusion of aluminum from the TiAl layer to the Ti64 layer, not only the volume fraction of the dark islands ( $\gamma$  phases, as indicated by A in Fig.5(a)) in Layer I decreased significantly, but also the

shape of the dark islands changed into needle shape ( $\gamma$  phases, as indicated by C in Fig.5(a)). In addition, from Fig.3 and Table 1, it can be found that vanadium elements contents in Layer I are more uniform than that in TiAl layer and still higher (14.09 at.%) than the composition of the TiAl alloy (8.8 at.%) due to the interdiffusion, which led to the increasing of the volume fraction of B2 phases in Layer I. It can be predicted that with increasing the number of rolling passes, the thickness of the interfacial region would increase. During cooling of the rolled laminate composite sheet after rolling, the  $\beta$  phase in Layer II was transformed into  $\alpha_2$  phase because of the high Al content in the range of 20-31 at.%, and in the meantime, following the Ti–Al–V ternary phase diagram [25], the  $\alpha$  phase and  $\beta$  phase in Layer I were changed into  $\gamma$  phase and B2 phase, respectively.

### ***3.2 Shear strength of the interfacial region***

To determine the bonding strength of the TiAl and Ti64 layers in the LMC sheet, the shear strength of the interfacial region was measured by conducting tensile testing using specimens with a designed shape as shown in Fig. 1 and Fig. 8(a). Using this test, it was determined that the ultimate shear strength of the specimens was 335.7MPa on average. The fracture morphology showed that the fracture occurred in TiAl layer as shown in Fig.8(b) and Fig.8(c), which reveals that the ultimate shear strength of the interfacial region was between those of the TiAl and Ti64 layers. This demonstrates that the bonding strength between the TiAl and Ti64 layers in the laminate composite sheet

is very high.

The following are the possible reasons for this high bonding strength between the TiAl and Ti64 layers:

(1) Both the TiAl layer and the Ti64 layer have same main elements (i.e. Ti, Al and V) and share a common phase which is  $\beta$  phase at the hot rolling temperature. This is helpful for fast atomic interdiffusion between the TiAl and Ti64 layers, leading to establishing strong interfacial bonding within a short time.

(2) For the laminate composite, if thermal expansion coefficient of different layer is quite different at high temperature, internal stress must be produced at the interface, which results in the decreasing of interface bonding strength [27]. Due to the same both disordered  $\beta$  phases and main elements of the TiAl and Ti64 layers during hot rolling, thermal expansion coefficient of the TiAl layer should be similar to that of Ti64 layer, indicating internal stress at the interfaces must be quite low.

(3) Because the strength of  $Ti_3Al$  intermetallic compound are better than that of TiAl intermetallic compound, the formation of  $Ti_3Al$  phases at the interface during the process of preparing the laminate composite sheet is very beneficial for enhancing the bonding strength between the TiAl and Ti64 layers.

As we know, TiAl alloys are a kind of brittle metallic materials. In order to toughen effectively composites with a brittle TiAl matrix, one important approach is to add a ductile phase which is required to have a strong interface with the matrix, which is very effective at improving toughness and plasticity. Weak interfacial bonding will lead to

the preferential crack initiation at interfaces, which can decrease the mechanical properties of the composites with a TiAl matrix. For the TiAl-Ti64 laminate composite, when a crack or a shear band impedes on the ductile Ti64 layer, a strong interface can ensure that the load transfer and the ductility of the Ti64 layer results in plastic energy dissipation. Obviously, the formation of a 250 $\mu$ m thick interdiffusion region successfully enhances the interfacial bonding between the TiAl and the Ti64 layers, which effectively transfers the stresses and strains to the ductile Ti64 layer resulting in continuous and extensive plastic deformation.

#### 4. Conclusions

1) Ti-6Al-4V/Ti-43Al-9V-Y laminate composite sheet with a uniform interfacial microstructure and no discernible defects at the interfaces has been prepared by hot-pack rolling at 1180°C. The thickness of TiAl-Ti64 LMC sheet was 2.9mm which corresponded to a total thick reduction of about 78%. The thickness of Ti-43Al-9V-Y alloy layer and Ti64 alloy layer was 2.3 and 0.6mm, respectively.

2) Microstructural examination reveals that there was an interfacial region of uniform thickness of about 250  $\mu$ m between the TiAl layer and the Ti64 layer of the LMC sheet. The interfacial region contained two layers: Layer I which was 80  $\mu$ m thick and Layer II which was 170  $\mu$ m thick. The microstructure of Layer I consisted of massive  $\gamma$  phases, needlelike  $\gamma$  phases and B2 phase matrix, while the microstructure of Layer II consisted of  $\alpha_2$  phase. The formation of the interfacial region was mainly

caused by the interdiffusion of Ti element from Ti64 layer into TiAl layer and Al element from TiAl layer into Ti64 layer.

3) The shear strength of the interfacial region is high, and this demonstrates that the bonding strength between the TiAl and Ti64 layers in the laminate composite sheet is quite high, and the interface is very effective in improving the toughness and plasticity of the Ti64-TiAl LMC sheet.

### Acknowledgements

This work was supported by the National Natural Science Foundation of China under Contract no. 51074058.

### References

- [1] J.H. She, T. Inoue, K. Ueno, Multilayer Al<sub>2</sub>O<sub>3</sub>/SiC ceramics with improved mechanical behavior. *J. Eur. Ceram. Soc.* 20 (2000) 1771-1775.
- [2] K.L. Hwu, B. Derby, Fracture of metal/ceramic laminates—I. Transition from single to multiple cracking. *Acta Mater.* 47 (1999) 529-534.
- [3] F. Carreno, J. Chao, M. Pozuelo, O.A. Ruano, Microstructure and fracture properties of an ultrahigh carbon steel–mild steel laminated composite. *Scr. Mater.* 48 (2003) 1135-1140.
- [4] M. Mitkov, D. Jankovic, D. Kicevic, Microstructure and strength of solid state bonded Ni-Al<sub>2</sub>O<sub>3</sub>-Ni<sub>3</sub>Al laminates. *Mater. Sci. Forum.* 282-283 (1998) 233-238.

- [5] A. Rohatgi, D.J. Harach, K.S. Vecchio, K.P. Harvey, Resistance-curve and fracture behavior of Ti–Al<sub>3</sub>Ti metallic–intermetallic laminate (MIL) composites. *Acta Mater.* 51 (2003) 2933-2957.
- [6] X.K. Peng, R. Wuhrer, G. Heness, W.Y. Yeung, On the interface development and fracture behaviour of roll bonded copperaluminum metal laminates. *J. Mater. Sci.* 34 (1999) 2029-2038.
- [7] E.J. Kubel Jr, Laminated metals provide tailor-made properties. *Mater. Eng.* 102 (1985) 23-26.
- [8] K.L. Hwu, B. Derby, Fracture of metal/ceramic laminates—II. Crack growth resistance and toughness. *Acta Mater.* 47 (1999) 545-563.
- [9] T.Z. Li, F. Grignon, D.J. Benson, K.S. Vecchio, E.A. Olevsky, F.J. Jiang, Modeling the elastic properties and damage evolution in Ti–Al<sub>3</sub>Ti metal–intermetallic laminate (MIL) composites. *Mater. Sci. Eng. A.* 374 (2004) 10-26.
- [10] J.G. Luo, V.L. Acoff, Using cold roll bonding and annealing to process Ti/Al multilayered composites from elemental foils. *Mater. Sci. Eng. A.* 379 (2004) 164-172.
- [11] N. Masahashi, S. Watanabe, N. Nomura, S. Semboshi, S. Hanada, Laminates based on an iron aluminide intermetallic alloy and a CrMo steel. *Intermetallics.* 13 (2005) 717-726.
- [12] T.T. Ueda, M. Tsukahara, Y. Kamiya, S. Kikuchi, Preparation and hydrogen storage properties of Mg–Ni–Mg<sub>2</sub>Ni laminate composites. *J. Alloy Compd.* 386 (2005)



253-257.

- [13] Huiyu Sun, Ning Pan, Mechanical characterization of the interfaces in laminated composites. *Composite Structures*. *Compos. Struct.* 74 (2006) 25-29.
- [14] W.O. Soboyejo, F. Yea, L.C. Chena, N. Bahtishia, D.S. Schwartz, R.J. Lederich, Effects of reinforcement morphology on the fatigue and fracture behavior of  $\text{MoSi}_2/\text{Nb}$  composites. *Acta Mater.* 44 (1996) 2027-2041.
- [15] Y.M. Hwang, H. Hsu, Y. Hwang, Analytical and experimental study on bonding behavior at the roll gap during complex rolling of sandwich sheets. *Int. J. Mech. Sci.* 42 (2000) 2417-2437.
- [16] R. V. Ramanujan, Phase transformations in  $\gamma$  based titanium aluminides. *International Mater. Rev.* 45 (2000) 217-240.
- [17] Yuyong Chen, Yanfei Chen, Fantao Kong, Shulong Xiao, Fabrication and processing of gamma titanium aluminides - A review. *Mater. Sci. Forum.* 638-642 (2010) 1281-1287.
- [18] Xinhua Wu, Review of alloy and process development of TiAl alloys. *Intermetallics*. 14 (2006) 1114-1122.
- [19] D.J. Goda, N.L. Richards, W.F. Caley, M.C. Chaturvedi, The effect of processing variables on the structure and chemistry of Ti-aluminide based LMCS. *Mater. Sci. Eng. A.* 334 (2002) 280-290.
- [20] T. Li, F. Jiang, E.A. Olevsky, K.S. Vecchio, M.A. Meyers, Damage evolution in  $\text{Ti6Al4V-Al}_3\text{Ti}$  metal–intermetallic laminate composites. *Mater. Sci. Eng. A.* 443

(2007) 1-15.

- [21] Tiezheng Li, Eugene Al Olevsky, Marc Andre Meyers, The development of residual stresses in Ti6Al4V-Al<sub>3</sub>Ti metal-intermetallic laminate (MIL) composites. *Mater. Sci. Eng. A.* 473 (2008) 49–57.
- [22] G.Y. Tzou, A.K. Tieu, M.N. Huang, C.Y. Lin, E.Y. Wu, Analytical approach to the cold and-hot bond rolling of sandwich sheet with outer hard and inner soft layers. *J. Mater. Proc. Technol.* 125-126 (2002) 664-669.
- [23] Fantao Kong, Yuyong Chen, Preparation of  $\gamma$ -TiAl/TC4 composite sheet and its microstructure and properties. *Rare Met. Mater. Eng.* 38 (2009) 1484-1486.
- [24] Fantao Kong, Yuyong Chen, Evolution of the microstructure of as-rolled Ti-43Al-9V-Y alloy with different heat treatments. *TMS 2009 Annual Meeting - 138th Annual Meeting and Exhibition - Supplemental Proceedings.* 3 (2009) 593-599.
- [25] Masao Takeyama, Satoru Kobayashi, Physical metallurgy for wrought gamma titanium aluminides Microstructure control through phase transformations. *Intermetallics.* 13 (2005) 993–999.
- [26] D.J. Goda, N.L. Richards, W.F. Caley, M.C. Chaturvedi, The effect of processing variables on the structure and chemistry of Ti-aluminide based LMCS. *Mater. Sci. Eng. A.* 334 (2002) 280-290.
- [27] W.J. Zhang, B.V. Reddy, S.C. Deevi, Physical properties of TiAl-base alloys. *Scr. Mater.* 45 (2001) 645-651.

## Figure captions

**Fig.1** interface shear test sample.

**Fig.2** SEM backscattered electron images showing the microstructures of (a) TiAl alloy layer and (b) Ti-6Al-4V alloy layer of the LMC sheet.

**Fig.3** (a) SEM backscattered electron image of the interfacial region of the cross-section of the laminate composite; and (b) distribution of the contents of Ti, Al and V along Line A-B shown in (a).

**Fig.4** XRD pattern of cross-section of the laminate composite.

**Fig.5** SEM backscattered electron images of the microstructures of (a) Layer I and (b) Layer II of the interfacial region between the TiAl and Ti64 layers.

**Fig.6** TEM bright field images of the microstructures of (a) Layer I and (b) Layer II of the interfacial region of the laminate composite.

**Fig.7** The schematic diagram of the structure of the interfacial region of the laminate composite sheet.

**Fig. 8** (a) Images showing the side view and top view of specimens used in the tensile testing; (b) Image showing the top view of the specimen after fracture; (c) The schematic diagram of the side view of the specimen after fracture.

**Table caption**

**Table 1** EDS analysis results from the points shown in Fig. 5

ACCEPTED MANUSCRIPT

**Table**

Table 1 EDS analysis results from the points shown in Fig. 5

Position number	Ti (at.%)	Al (at.%)	V (at.%)	Possible phases
A	49.96	44.33	5.72	$\gamma$
B	49.83	43.26	6.91	$\gamma$
C	48.70	46.21	5.09	$\gamma$
D	54.25	31.66	14.09	B2
E	62.02	31.36	6.38	$\alpha_2$
F	68.98	26.55	4.48	$\alpha_2$
G	75.33	20.57	4.09	$\alpha_2$
H	82.43	11.20	6.37	$\alpha+\beta$

## Figures

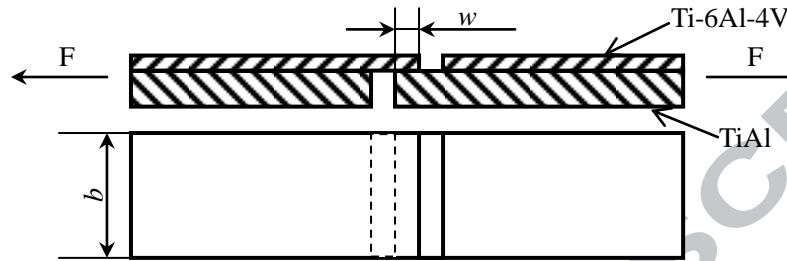


Fig.1 interface shear test sample.

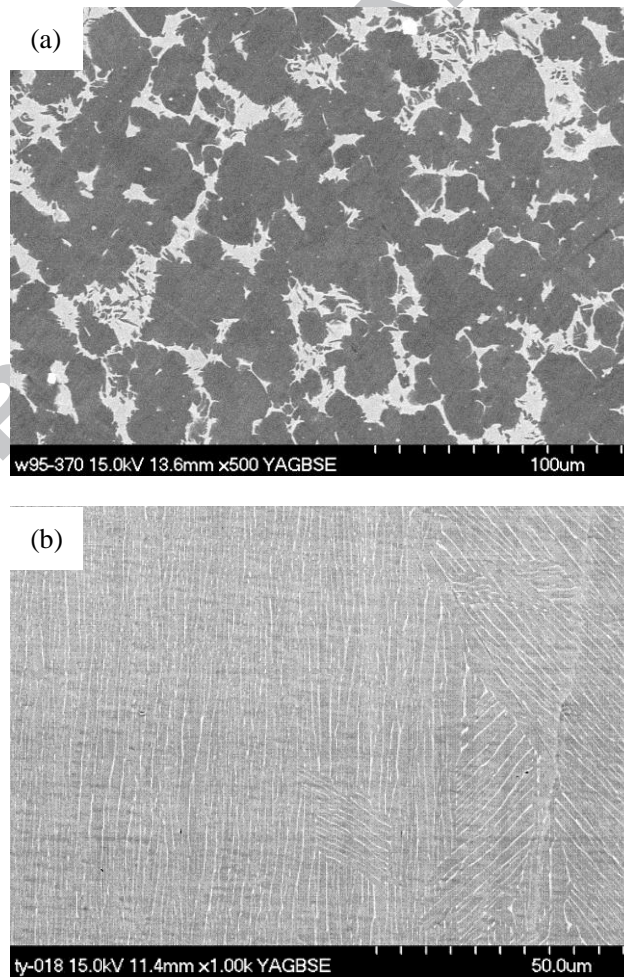


Fig.2 SEM backscattered electron images showing the microstructures of (a) TiAl alloy layer and (b) Ti-6Al-4V alloy layer of the LMC sheet.

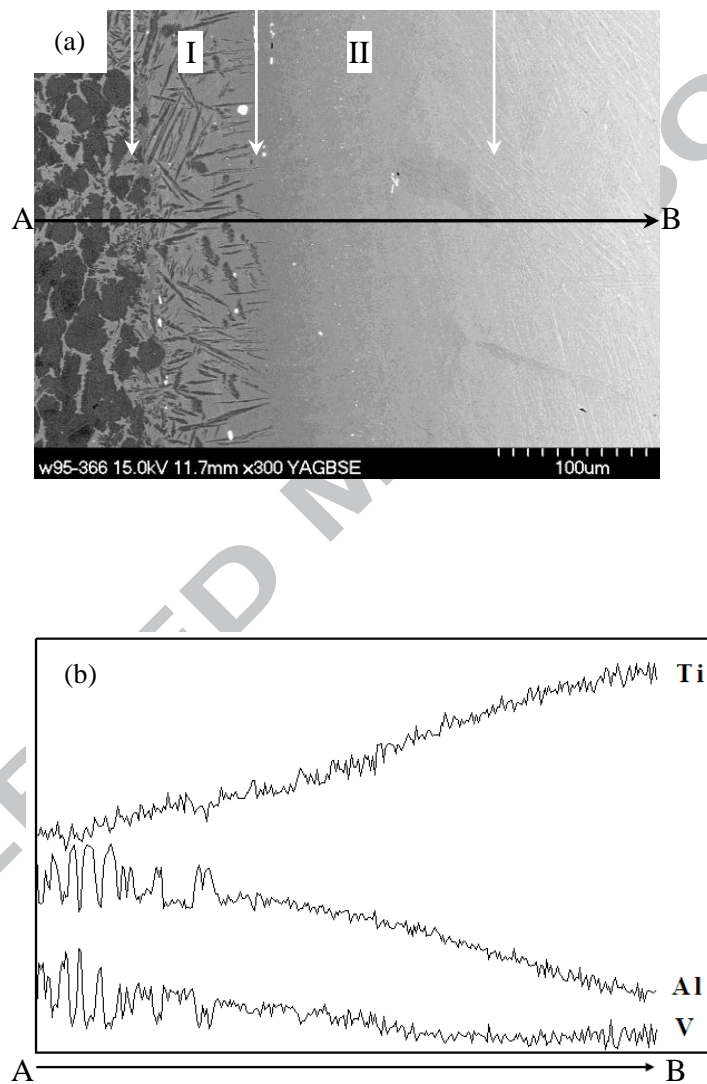


Fig.3 (a) SEM backscattered electron image of the interfacial region of the cross-section of the laminate composite; and (b) distribution of the contents of Ti, Al and V along Line A-B shown in (a).

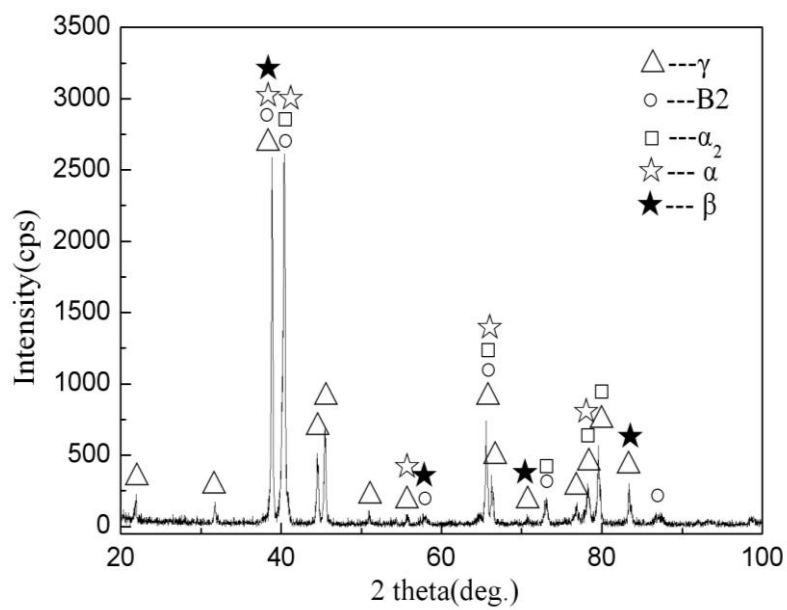


Fig.4 XRD pattern of cross-section of the laminate composite.



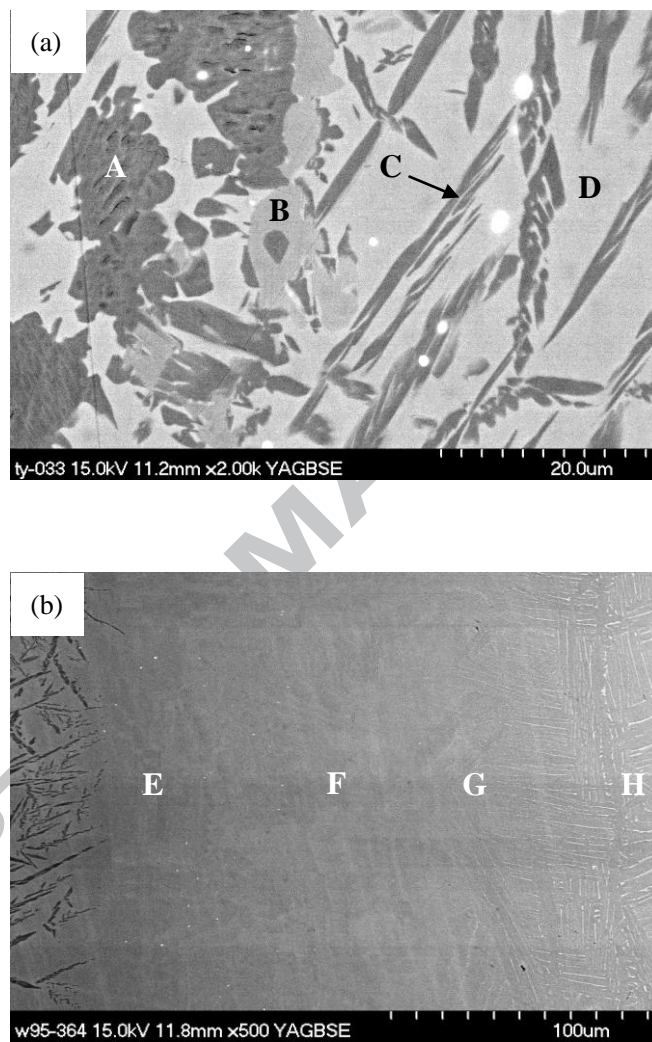


Fig.5 SEM backscattered electron images of the microstructures of (a) Layer I and (b) Layer II of the interfacial region between the TiAl and Ti64 layers.

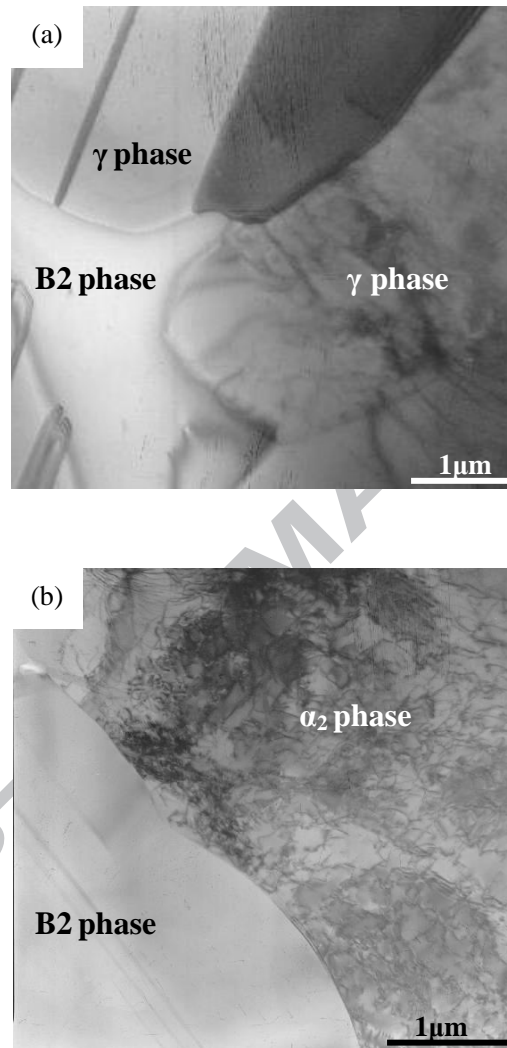


Fig.6 TEM bright field images of the microstructures of (a) Layer I and (b) Layer II of the interfacial region of the laminate composite.

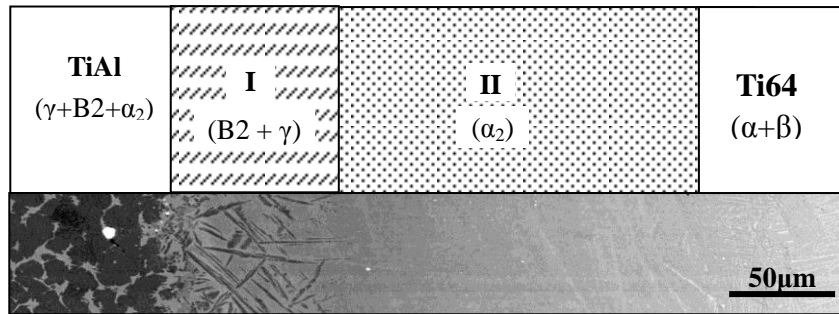


Fig.7 The schematic diagram of the structure of the interfacial region of the laminate composite sheet.

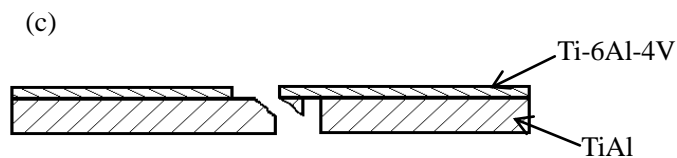
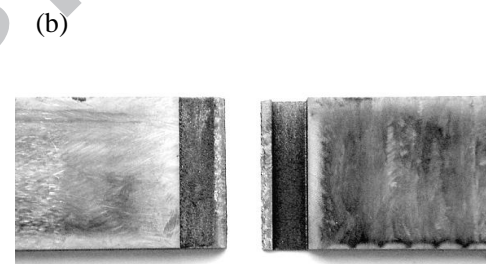
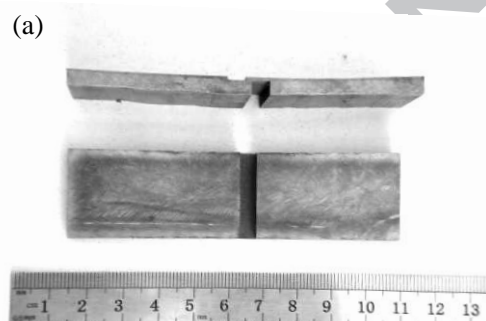


Fig. 8 (a) Images showing the side view and top view of specimens used in the tensile testing; (b) Image showing the top view of the specimen after fracture; (c) The schematic diagram of the side view of the specimen after fracture.

### Research Highlights

- Ti6Al4V/TiAl laminate composite sheet has been prepared by hot-pack rolling.
- There was an interfacial region between the TiAl and the Ti6Al4V layers.
- The bonding strength between the TiAl and Ti6Al4V layers is quite high.